energies

MDPI

Article

Techno-Economic Comparison of Data Center Cooling Using Magnetic Bearing Chillers and Aquifer Thermal Energy Storage

Apurva Malpure [1,*], Andrew Stumpf [2,*], Upasana Pandey [2], Yu-Feng Lin [2,3] and Craig Bradshaw [4]

[1] Department of Industrial & Enterprise Systems Engineering, University of Illinois Urbana-Champaign, Urbana, IL 61801, USA
[2] Illinois State Geological Survey, Prairie Research Institute, University of Illinois Urbana-Champaign, Champaign, IL 61820, USA; upandey@illinois.edu (U.P.); yflin@illinois.edu (Y.-F.L.)
[3] Illinois Water Resources Center, Prairie Research Institute, University of Illinois Urbana-Champaign, Champaign, IL 61820, USA
[4] Air-Conditioning and Refrigeration Center, Department of Mechanical Science & Engineering, University of Illinois Urbana-Champaign, Urbana, IL 61801, USA; crbrad@illinois.edu
* Correspondence: amalpu2@illinois.edu (A.M.); astumpf@illinois.edu (A.S.); Tel.: +1-217-721-7057 (A.M.); +1-217-244-6462 (A.S.)

Abstract

Data centers are large and rapidly growing electricity consumers, and cooling systems account for a substantial share of their energy demand. A key contribution of this study is a climate-sensitive, hourly techno-economic comparison of three data-center cooling configurations under consistent operating assumptions: a conventional water-cooled centrifugal chiller baseline, a magnetic bearing chiller (MBC) system, and an MBC system integrated with aquifer thermal energy storage (ATES). The comparison is performed for Phoenix, Arizona, and Fairbanks, Alaska, which represent substantially different cooling climates in the U.S. Hourly simulations use identical information technology (IT) load profiles, identical aggregate installed chiller capacity represented by two 4058 kW chiller units, common water-side economizer controls, and site-specific weather and electricity tariffs. Results show that the MBC system reduces annual cooling-system electricity consumption from 1169.4 to 957.4 MWh in Phoenix (18.1%) and from 361.6 to 319.4 MWh in Fairbanks (11.7%). Peak cooling-system electrical demand decreases by 119.4 kW in Phoenix and 71.6 kW in Fairbanks. Relative to the centrifugal baseline, the MBC case gives a 5.8-year simple payback in Phoenix but is not economically attractive in Fairbanks under the assumed tariff. The MBC-only case gives the lowest annual cooling electricity use in both climates. The MBC+ATES case is treated only as a screening-level, discharge-assisted cold-storage scenario rather than a full techno-economic assessment of seasonal ATES, and no site-specific hydrogeological feasibility assessment is performed. Under the assumed O&M cost structure, MBC+ATES gives a higher discounted value of savings than MBC-only, but this economic result is not caused by additional cooling-electricity savings relative to MBC-only. The MBC+ATES case also has a longer payback period because of its higher capital cost. These results show that the value of advanced cooling configurations depends on climate, free-cooling availability, electricity pricing, storage assumptions, and economic assumptions within the modeling framework considered in this study.

Keywords: underground thermal energy storage; techno-economic analysis; water-side economizer; cooling-only power usage effectiveness; AI infrastructure; geothermal energy; data center cooling

Check for updates

Academic Editor: Ioan Sarbu

Received: 25 June 2026
Revised: 19 August 2026
Accepted: 20 August 2026
Published: 22 August 2026

Copyright: © 2026 by the authors. Licensee MDPI, Basel, Switzerland. This article is an open access article distributed under the terms and conditions of the Creative Commons Attribution (CC BY) license.

1. Introduction

Data centers have become essential infrastructure for cloud computing, artificial intelligence (AI), high-performance computing, and other digital services. Their rapid expansion has increased electricity demand at national and global scales. In the U.S., data centers consumed approximately 176 TWh in 2023, corresponding to about 4.4% of national electricity demand. This demand is projected to increase to 325–580 TWh by 2028 [1]. Industry assessments also identify data-center growth as an important contributor to future electricity demand, especially as AI and high-density computing loads expand [2,3]. Recent U.S. market reporting identifies power availability as a major constraint on data-center expansion. This reinforces the need to evaluate cooling strategies that affect facility electrical demand [4].

Data-center cooling also has water-resource implications. Water can be consumed directly through evaporative cooling systems and indirectly through electricity generation. Previous studies have shown that data-center water use depends on cooling-system type, climate, electricity supply, server utilization, and local water stress [5–7]. Industry metrics such as water usage effectiveness (WUE) have also been proposed to evaluate data-center water performance alongside energy performance [8]. In the present study, water-related impacts are used only as contextual motivation for evaluating cooling electricity use and storage-assisted operation. Direct water consumption, cooling-tower makeup water, blowdown, evaporative losses, and source-energy water consumption are not quantified.

Cooling is one of the major non-IT electricity uses in data centers. Conventional chilled-water systems commonly use computer room air handler (CRAH) units, water-side economizers (WSEs), cooling towers, and water-cooled centrifugal chillers. These systems are mature and widely used. However, their annual energy performance depends strongly on outdoor weather conditions. When ambient wet-bulb temperatures are low enough, WSE operation can reduce or avoid mechanical cooling. In warmer periods or climates, the chiller must supply a larger fraction of the cooling load, which increases cooling electricity use. In this study, PUE′ is used as a cooling-only power usage effectiveness metric. It represents the ratio of IT electricity use plus cooling-system electricity use to IT electricity use. Therefore, it isolates the contribution of cooling equipment rather than representing whole-facility PUE. Climate and economizer availability are, therefore, essential when evaluating alternative cooling technologies [9].

Magnetic bearing chillers (MBCs) have been investigated as an alternative to conventional centrifugal chillers. They can reduce mechanical losses and improve part-load performance. Previous work has shown that MBC-based cooling systems can reduce data-center cooling energy use. However, the magnitude of the benefit depends on condenser-water temperature and the number of hours in which mechanical cooling is required [9]. As a result, MBC performance is strongly related to local climate and WSE availability.

Aquifer thermal energy storage (ATES), a form of underground thermal energy storage (UTES), has also been studied as a strategy for reducing cooling energy use and shifting thermal loads. ATES systems store thermal energy in aquifers and can provide cooling when ambient or system conditions make direct heat rejection less favorable. Reviews and techno-economic studies show that ATES performance depends on storage sizing, hydrogeologic conditions, well design, pumping energy, and operating strategy [10–12]. Studies of data-center cooling have also examined the potential role of UTES for reducing cooling demand and managing waste heat [13–15]. ATES is considered a scalable heating and cooling technology that may be suited to the evolving cooling needs of data centers [16]. Recent assessments further emphasize that ATES deployment depends on suitable aquifers, heating and cooling demand, and improved design and operating practices [17]. Technical reports also describe ATES as a seasonal storage approach using paired warm and cold

wells. Its performance depends on subsurface conditions, well design, and operational control [18].

Despite these developments, many studies evaluate advanced chillers, WSE operation, and thermal storage as separate measures. Fewer studies assess how these measures interact within a common hourly framework for data-center cooling. This gap is especially important when comparing contrasting climates under identical IT-load assumptions. The importance of an efficient chiller depends on the frequency with which the chiller operates. The Importance of an ATES-assisted case also depends on storage assumptions, pumping requirements, dispatch logic, and whether seasonal charging is represented. A consistent comparison requires equal rated chiller capacity and weather inputs that represent wet-bulb conditions rather than dry-bulb temperature alone. The novelty of this study is the combined hourly techno-economic comparison of a centrifugal baseline, an MBC system, and a screening-level MBC+ATES configuration under identical IT-load, chiller-capacity, wet-bulb, and economic assumptions for two contrasting U.S. climates.

Table 1 summarizes how the present study is positioned relative to selected previous studies on magnetic bearing chillers, data-center cooling, and subsurface thermal energy storage.

Table 1. Comparison of the present study with selected previous studies on data-center cooling, magnetic bearing chillers, and subsurface thermal energy storage.

Study	Focus and Relation to the Present Study
Dai et al. [9]	Studied magnetic bearing chillers and water-side economizer retrofits for data-center cooling, including energy and economic comparisons across different climate cities in China. The present study extends this direction by adding an MBC+ATES case and comparing two contrasting U.S. climates.
Oh et al. [1]	Evaluated reservoir thermal energy storage for data-center cooling using dry coolers and heat recovery for a year-round cooling load. The present study instead evaluates a simplified ATES-assisted configuration coupled with magnetic bearing chillers.
Zhang et al. [14]	Assessed subsurface thermal energy storage for data-center cooling, with a focus on technical feasibility for a representative data-center application in Houston, Texas. The present study adds hourly cooling-system dispatch and economic comparison for Phoenix and Fairbanks.
Dvorak et al. [13]	Simulated data-center waste heat utilization with an existing campus ATES system. The present study focuses on cooling-electricity and economic outcomes for centrifugal, MBC, and MBC+ATES configurations.
Fleuchaus et al. [10]	Reviewed global ATES deployment, energy savings, costs, and barriers. The present study applies ATES as a screening-level cooling-support option for data-center cooling.
Schüppler et al. [11]	Presented a techno-economic and environmental analysis of ATES for heating and cooling in Germany. The present study applies a similar techno-economic perspective to data-center cooling configurations.

This study addresses the identified gap by developing an hourly techno-economic framework to compare three data-center cooling configurations. The configurations are as follows: (i) a baseline water-cooled centrifugal chiller system with WSE and CRAH units, (ii) an MBC system with WSE and CRAH units, and (iii) a screening-level MBC+ATES configuration. The analysis is conducted for Phoenix, Arizona, and Fairbanks, Alaska. These cities represent contrasting hot-dry and cold-continental climatic conditions in the U.S.. They are used as climate-representative cases rather than as confirmed ATES deployment sites. Both sites are evaluated using identical IT load profiles, equal chiller capacity, humidity-based outdoor wet-bulb calculations, and consistent operating assumptions.

The objective is to quantify how climate and system configuration influence annual cooling electricity consumption, cooling-only PUE′, peak cooling-system electrical demand, and economic metrics. The economic metrics include simple payback period and discounted value of savings. Throughout this manuscript, PUE′ refers only to IT load and cooling-system electricity use. Other facility loads, such as lighting, power distribution losses, and non-cooling auxiliary systems, are excluded. The results are intended as comparative outcomes within the defined modeling framework. They are not intended as universal design recommendations for a specific facility. A list of abbreviations and symbols used in the manuscript is provided in Appendix 5.

2. Materials and Methods

2.1. Assumptions and Boundary Conditions

For this study, an integrated techno-economic framework couples an hourly cooling-system dispatch model with a financial evaluation module. The framework is used to compare annual cooling energy use, electrical demand during peak cooling, cooling-only PUE′, and project-level economic metrics under a consistent set of modeling assumptions.

Three cooling configurations are evaluated: (i) a baseline water-cooled centrifugal chiller plant with water-side economizer (WSE) and computer room air handler (CRAH) units, (ii) a magnetic bearing chiller (MBC) plant with WSE and CRAH units, and (iii) an MBC plant integrated with aquifer thermal energy storage (ATES). For the ATES case, dispatch priority follows the WSE → ATES → chiller so that lower-energy cooling sources are used before mechanical cooling.

The centrifugal and magnetic bearing chiller cases are modeled with identical aggregate installed chiller capacity. Each configuration uses two 4058 kW chiller units, giving a total installed chiller-plant capacity of 8116 kW. The two chiller units are represented as an equivalent aggregate chiller plant rather than as individually staged machines. Therefore, the part-load ratio is calculated as the hourly mechanical cooling load divided by the total installed chiller capacity. The COP correlation is evaluated using this aggregate part-load ratio and the condenser/tower-water temperature. Explicit unit staging, minimum individual chiller loading, and lead–lag control are not modeled. No additional standby or N+1 redundancy capacity is included beyond the two modeled units. This aggregate representation is used consistently for the centrifugal and magnetic bearing chiller cases so that the comparison is not biased by different capacity or redundancy assumptions. This capacity matching ensures that the differences in the predicted performance arise from variations in the coefficient of performance (COP), auxiliary loads, controls, climate, and cost assumptions rather than from dissimilar equipment sizing. The temperature of the supplied chilled water is fixed at 7 °C, with a temperature difference of 5 K. The performance of the cooling tower is represented using a 4 K approach temperature and a minimum condenser/tower-water temperature of 2 °C. The condenser/tower-water temperature available to the WSE and chiller condenser side is calculated as:

$$T_{ctw,h} = \max\left(T_{wb,out,h} + \Delta T_{app},\ T_{ctw,min}\right) \quad (1)$$

where $T_{ctw,h}$ is the temperature of condenser/tower water after heat rejection from the cooling tower, $T_{wb,out,h}$ is the outdoor wet-bulb temperature, ΔT_{app} is the temperature of cooling tower water upon approach, and $T_{ctw,min}$ is the minimum temperature allowed for the condenser/tower water.

The ATES case is represented as a screening-level, discharge-assisted storage configuration rather than a complete seasonal ATES design. The storage reservoir has a maximum capacity of 400 MWh_{th} and a maximum discharge rate of 5000 kW_{th}. The initial state of charge is set to 50% of the maximum storage capacity. Charging is not represented in the

base case. This assumption isolates the effect of using available cold storage to offset chiller operation under the selected storage size and dispatch logic.

The standing loss of the ATES is specified as a monthly loss fraction, $\lambda_m = 0.02$, and converted to an equivalent hourly loss fraction. The assumed well depth is 80 m, with five cold wells and five warm wells. The borefield representation is a simplified feasibility-level configuration rather than a site-specific hydrogeological design. This level of detail is consistent with early-stage feasibility screening, but it should not be interpreted as a final seasonal ATES design [19]. Site-specific cold- and warm-well temperatures are prescribed as 6 °C and 15 °C for Phoenix, and 3 °C and 12 °C for Fairbanks. The cities of Phoenix and Fairbanks are used here as representative contrasting cooling climates rather than as site-specific ATES deployment locations. Therefore, the prescribed ATES parameters should be interpreted as hypothetical screening assumptions, not as evidence of hydrogeological feasibility or actual deployability in either city.

All simulations use hourly time steps for one calendar year. Cooling loads, heat-transfer rates, storage energy, flow rates, and electrical powers are constrained to non-negative values. The ATES state of charge is bounded by $0 \leq E_h \leq E_{\max}$, and discharge is limited by both the available stored energy and the maximum discharge rate.

2.2. System Description

The modeled cooling system follows a conventional chilled-water architecture consisting of CRAH units, chilled-water pumps, condenser-water pumps, cooling towers, a plate heat exchanger for water-side economizer operation, and water-cooled mechanical chillers. In all configurations, CRAH units remove heat from the data center space and transfer it to the chilled-water loop. The WSE provides free cooling when outdoor wet-bulb conditions allow heat rejection through the cooling tower without mechanical compression. Mechanical chillers meet any remaining load that cannot be satisfied by WSE operation and, in the ATES case, by storage discharge.

The WSE heat-transfer rate is calculated using an effectiveness method that accounts for the number of transfer units (NTU):

$$Q_{wse,h} = \varepsilon_h C_{\min,h} \max(0,\ T_{cw,r,h} - T_{ctw,h}) \tag{2}$$

where $Q_{wse,h}$ is the cooling rate of the WSE, ε_h is the heat-exchanger effectiveness, $C_{\min,h}$ is the smaller heat capacity of the chilled water and condenser water streams, $T_{cw,r,h}$ is the temperature of the returned chilled water and $T_{ctw,h}$ is the temperature of the condenser water entering the WSE. The rate of heat transfer is capped so that it does not exceed the hourly cooling load or overcool the chilled-water stream below the supply setpoint.

The operating mode of the energy system is assigned from the calculated WSE contribution:

$$\text{Mode}_h = \begin{cases} \text{Full free cooling}, & Q_{wse,h} \geq Q_{sum,h} \\ \text{Partial free cooling}, & 0 < Q_{wse,h} < Q_{sum,h} \\ \text{Mechanical cooling}, & Q_{wse,h} = 0 \end{cases} \tag{3}$$

where $Q_{sum,h}$ is the total hourly cooling load.

2.3. Data Inputs and Parameters

All inputs to the model are structured as 8760-hour annual time series for the cities of Phoenix and Fairbanks. The Phoenix area represents a hot dry climate, while Fairbanks represents a cold continental climate. The two sites use identical IT load profiles so that differences in results are driven by weather, humidity, tariff, and system-response differences rather than by different server-load assumptions. The processed hourly input profiles

used for Phoenix and Fairbanks are provided in the Supplementary Materials. These files include the hourly date/time, server load, indoor wet-bulb temperature, outdoor dry-bulb temperature, and relative humidity used in the simulations.

2.3.1. Weather and Humidity Data

The hourly outdoor dry-bulb temperature data for 2022 are obtained from WeatherSpark for the two cities [20,21]. Hourly relative humidity data are obtained from Weather Underground historical observations for the Phoenix Sky Harbor International Airport (KPHX) and Ladd Army Airfield at Fort Wainwright (PAFB) [22,23]. The relative-humidity record is paired with the corresponding hourly dry-bulb temperature series. For short time periods without humidity measurements, the data are extrapolated from a linear interpolation before the wet-bulb calculation.

The outdoor wet-bulb temperature $T_{wb,out,h}$ is calculated from the hourly dry-bulb temperature, relative humidity, and estimated site pressure. Site pressure is estimated from elevation using the standard barometric relationship:

$$p = 101.325\left(1 - 2.25577 \times 10^{-5} z\right)^{5.2559} \tag{4}$$

where p is the atmospheric pressure in kPa and z is the surface elevation at the site in m.

A commonly used closed-form approximation for wet-bulb temperature from dry-bulb temperature and relative humidity is given by Stull [24]:

$$\begin{aligned} T_{wb} \approx T_{db} \tan^{-1}\left[0.151977(RH + 8.313659)^{1/2}\right] + \tan^{-1}(T_{db} + RH) \\ - \tan^{-1}(RH - 1.676331) + 0.00391838 RH^{3/2} \tan^{-1}(0.023101 RH) - 4.686035 \end{aligned} \tag{5}$$

where T_{wb} and T_{db} are in °C, and RH is the relative humidity in percent. This equation is included to show the physical dependence of wet-bulb temperature on both dry-bulb temperature and humidity.

In the simulation implementation, $T_{wb,out,h}$ is calculated using a thermodynamic psychrometric solution rather than the Stull closed-form approximation. The calculation uses dry-bulb temperature, relative humidity, and site pressure to determine the moist-air state, then solves for the saturated-air temperature with equivalent moist-air enthalpy. The saturated vapor pressure is evaluated using the Buck formulation [25], and the thermodynamic wet-bulb calculation follows standard psychrometric relationships [26]. The resulting hourly data $T_{wb,out,h}$ are used in the calculations for the cooling tower, WSE, and the condenser water from the chiller.

2.3.2. IT Load Profile

The IT load profile is derived from the DOE OpenEI commercial reference building hospital electricity profile [27]. The source profile is not used directly as a hospital load in the cooling model. It is used only to provide normalized hourly temporal variation. After normalization, the profile is rescaled to a representative data-center IT-load range. The minimum load is set to approximately 80% of the annual peak so that the profile remains relatively flat, as expected for high-load-factor data-center server operation, while still retaining hourly variation. This transformation avoids the unrealistically low part-load hours that would result from applying the original building profile directly. The resulting profile ranges from 1269.9 to 1587.4 kW, with an annual mean of 1412.7 kW. The same server-load profile is used for Phoenix and Fairbanks so that differences in cooling performance are driven by climate and cooling-system operation rather than by different IT-load schedules.

Thus, the transformed profile is used as a representative high-load-factor screening input rather than as a measured IT-load trace from a specific data center.

The transformed load is represented as follows:

$$P_{IT,h} = P_{min} + \frac{P_{raw,h} - P_{raw,min}}{P_{raw,max} - P_{raw,min}} \left(P_{peak} - P_{min} \right) \quad (6)$$

where $P_{raw,h}$ is the original hourly reference-building load, $P_{raw,min}$ and $P_{raw,max}$ are the minimum and maximum values of the original annual profile, P_{peak} is the selected peak IT load of the data center, and $P_{min} = 0.8P_{peak}$. The 80% floor is imposed after normalizing the source profile and represents the lower bound of the modeled high-load-factor IT operation.

The hourly IT electrical load is converted to an equivalent IT heat load as shown:

$$Q_{IT,h} = P_{IT,h} \quad (7)$$

where $Q_{IT,h}$ is in kW_{th} and $P_{IT,h}$ is in kW_e. This relationship assumes that nearly all electricity used for IT processes is converted to heat and dissipated within the data center.

The auxiliary internal heat gains are represented as 10% of the heat generated from the IT processes:

$$Q_{aux,h} = 0.10Q_{IT,h} \quad (8)$$

The 0.10 (10%) term represents additional internal heat added to the cooling load. It is not used as a substitute for cooling-system auxiliary electrical power, which is calculated separately for CRAH fans, pumps, cooling-tower fans, and ATES pumping where applicable. The total hourly cooling load is, therefore, the following:

$$Q_{sum,h} = Q_{IT,h} + Q_{aux,h} \quad (9)$$

2.3.3. Indoor Environmental Conditions

The indoor wet-bulb temperature is treated as a controlled data-center operating variable. In the hourly input profile, $T_{wb,in}$ is bounded between 12 °C and 14 °C to represent controlled indoor humidity conditions. These environmental conditions are retained as an input descriptor, while the outdoor wet-bulb temperature is calculated separately from the outdoor dry-bulb temperature and relative humidity values for WSE and cooling tower dispatch. The auxiliary equipment was modeled using rated component capacities and load-dependent operating relationships. The rated parameters used for the CRAH fans, chilled-water pumps, condenser-water pumps, cooling-tower fans, and ATES well pumps are summarized in Table 2.

Table 2. Auxiliary-equipment parameters used in the cooling-system power model.

Component	Rated Parameter	Operating Representation
CRAH fans	113 CRAH units; total fan power 524.6 kW	Fan power scales with the cube of the cooling-load fraction.
Chilled-water pumps	Two pumps; 660 m^3/h and 75 kW per pump	Pump power scales with the cube of the chilled-water flow fraction.
Condenser-water pumps	Two pumps; 900 m^3/h and 55 kW per pump	Pump power scales with the cube of the condenser-water flow fraction.
Cooling-tower fans	Two tower cells; 37.5 kW per cell	Fan power scales with the cube of the heat-rejection-load fraction.
ATES well pumps	5000 kW_{th} maximum discharge; 80 m well depth	Pumping power is included during ATES discharge.

2.4. Chiller and Auxiliary Power Model

The part-load ratio of the chiller is calculated using the following:

$$PLR_h = \frac{Q_{chiller,h}}{Q_{cap,total}} \tag{10}$$

where $Q_{chiller,h}$ is the hourly mechanical cooling load and $Q_{cap,total}$ is the total capacity of the chiller. The value of PLR_h is between 0 and 1 for evaluating the COP.

Although the partial-load ratio is used in the chiller-performance calculation, the comparison is not based on a part-load-factor-only correction. Instead, centrifugal and magnetic bearing chillers are evaluated using separate COP surfaces that depend on both the temperature of the condenser water and the partial-load ratio. This evaluation allows the development of a model that captures both climate-driven condenser-water effects and technology-specific part-load performance.

The centrifugal chiller COP is calculated as follows:

$$COP_{cen,h} = b_1 + b_2 T_{ctw,h} + b_3 PLR_h + b_4 T_{ctw,h}^2 + b_5 T_{ctw,h} PLR_h + b_6 PLR_h^2 \tag{11}$$

The magnetic bearing chiller COP is calculated as follows:

$$COP_{mbc,h} = c_1 + c_2 T_{ctw,h} + c_3 PLR_h + c_4 T_{ctw,h}^2 + c_5 T_{ctw,h} PLR_h + c_6 PLR_h^2 \tag{12}$$

The centrifugal coefficients are $(b_1, b_2, b_3, b_4, b_5, b_6) = (25.47, -1.066, 6.335, 0.01188, 0.1263, -7.581)$, and the MBC coefficients are $(c_1, c_2, c_3, c_4, c_5, c_6) = (25.17, -0.7536, -1.081, 0.005736, 0.1851, -4.568)$ [9]. In these fitted COP surfaces, $T_{ctw,h}$ is the condenser-water temperature in °C, PLR_h is dimensionless, and COP is dimensionless. COP values are bounded between 2 and 18 as a numerical safeguard for polynomial extrapolation. The upper bound is not a nominal rated COP. It limits extrapolated values under very low condenser-water temperature and low part-load conditions. This range is consistent with the high low-temperature COP values reported for magnetic bearing chillers in the source study [9]. The lower bound was not reached in any simulated chiller-operating hour. The upper bound was reached mainly during cold-climate, low-lift operation when the remaining mechanical chiller load after free cooling was small. For significant-load operation, the upper bound had limited influence. In Fairbanks, the centrifugal chiller did not reach the upper bound in any hour with significant chiller load, and the MBC case reached the upper bound for only 27 h, corresponding to approximately 0.3% of the year. Therefore, the upper bound primarily prevents unrealistically high extrapolated COP values during low-temperature operating periods rather than controlling the main annual energy results.

The hourly electricity usage is as follows:

$$P_{chiller,h} = \frac{Q_{chiller,h}}{COP_h} \tag{13}$$

CRAH fans, chilled-water pumps, condenser-water pumps, and cooling-tower fans are modeled using cubic variable-speed scaling based on standard pump and fan affinity laws [28]:

$$P_{aux,i,h} = P_{aux,i,rated} f_{i,h}^3 \tag{14}$$

where $f_{i,h}$ is the normalized flow or load fraction for i. The total power required for the cooling system is determined by the following:

$$P_{cooling,h} = P_{chiller,h} + P_{CRAH,h} + P_{CHW,h} + P_{CTW,h} + P_{tower,h} + P_{ATES,h} \tag{15}$$

where $P_{ATES,h}$ is included only when the ATES is operated.

The hourly cooling-only power usage effectiveness is calculated as follows:

$$PUE'_h = 1 + \frac{P_{cooling,h}}{P_{IT,h}}, \tag{16}$$

where $P_{cooling,h}$ is the total cooling-system electrical power at hour h and $P_{IT,h}$ is the IT electrical load at hour h. The annual value reported in the results is the average of PUE'_h over all 8760 hourly timesteps. This metric is not the conventional whole-facility PUE because it excludes lighting, power distribution losses, and other non-cooling facility loads.

2.5. ATES Dispatch and Storage Balance

For the MBC+ATES case, the remaining energy load beyond operating the WSE is equal to the following:

$$Q_{need,h} = \max(0, Q_{sum,h} - Q_{wse,h}) \tag{17}$$

Discharge water from the ATES is only available when the storage-side temperature can provide useful cooling through the heat exchanger. The hourly ATES discharge is as follows:

$$Q_{ates,h} = \min\left(Q_{need,h}, q_{max}, \frac{E_h}{\Delta t}\right) \tag{18}$$

where q_{max} is the maximum ATES discharge rate and E_h is the thermal energy stored available at the beginning of each hour of operation h.

The monthly standing-loss fraction is converted to an equivalent hourly loss fraction using:

$$\lambda_h = 1 - (1 - \lambda_m)^{1/720} \tag{19}$$

where $\lambda_m = 0.02$ and 720 is the number of hours in a 30-day month. The storage balance is then the following:

$$E_{h+1} = \max[0, (E_h - Q_{ates,h}\Delta t)(1 - \lambda_h)] \tag{20}$$

The remaining load met by mechanical cooling is as follows:

$$Q_{chiller,h} = \max(0, Q_{need,h} - Q_{ates,h}) \tag{21}$$

2.6. Hourly Simulation Workflow

For each hourly timestep, the model considers IT electricity load, outdoor dry-bulb temperature, relative humidity, and indoor wet-bulb temperature. The outdoor wet-bulb temperature is calculated from the dry-bulb temperature, relative humidity, and estimated site pressure. The cooling tower outlet temperature is then determined from the outdoor wet-bulb temperature and tower approach. The total cooling load is calculated from the IT load and auxiliary heat allowance, and the WSE heat-transfer rate is evaluated using the effectiveness–NTU heat-exchanger model.

At each hourly timestep, the model first calculates the cooling supplied by the water-side economizer (WSE). Any cooling load not met by the WSE is treated as the remaining load. For the centrifugal and MBC-only cases, this remaining load is supplied entirely by the mechanical chiller. For the MBC+ATES case, the model first uses available ATES cooling, subject to the storage state of charge, maximum discharge rate, and heat-exchanger temperature constraints. Any load that still remains after ATES discharge is then supplied by the mechanical chiller. The chiller coefficient of performance (COP) is calculated from the condenser-water temperature and the chiller part-load ratio using the appropriate technology-specific COP surface. The model then calculates hourly chiller power, auxiliary power, total cooling-system power, and cooling-only PUE′. These hourly results are

aggregated to determine annual cooling electricity consumption, peak cooling-system electrical demand, and financial inputs. The overall hourly simulation and methodological workflow is summarized in Figure 1.

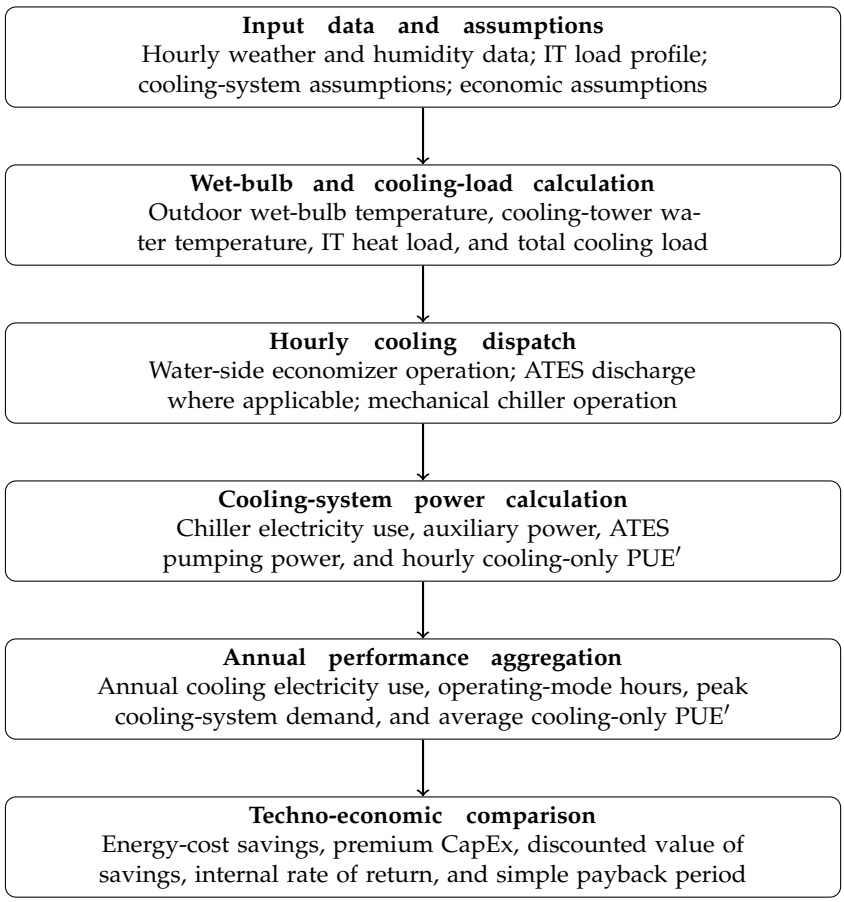


Figure 1. Methodological workflow used for the hourly cooling-system simulation and techno-economic comparison.

2.7. Financial Evaluation

The financial analysis is formulated as a screening-level relative comparison among the three cooling configurations. It is not intended to represent a site-specific procurement estimate or a complete project-finance model. The same economic framework is applied to both cities and all configurations so that differences in the results can be attributed to cooling energy use, local electricity tariff, capital cost, and modeled O&M assumptions. Similar simplified techno-economic comparisons are commonly used for early-stage evaluation of data-center cooling and ATES systems [9,11,12].

Electricity tariffs are modeled as flat energy rates of 0.10 $/kWh for Phoenix and 0.08 $/kWh for Fairbanks. The financial calculations assume a 20-year project life, a real discount rate of 5%, and a real annual electricity-price escalation rate of 2%. Demand charges, time-of-use rates, tax effects, financing structure, and site-specific utility incentives are not included in the base case. These exclusions keep the comparison consistent across climates and configurations, but they also limit the interpretation of the economic results.

Peak cooling-system demand reductions are reported as technical performance metrics in this study, but they are not monetized in the base financial analysis. Monetizing these reductions would require utility-specific demand-charge structures, time-of-use schedules, ratchet provisions, and data-center-specific tariff agreements. Therefore, the financial results should be interpreted as energy-charge-based screening estimates rather than complete utility-bill estimates. The financial evaluation uses a screening-level set of electricity-

price, discount-rate, escalation-rate, project-life, capital-cost, and O&M assumptions, as summarized in Table 3.

Table 3. Economic assumptions used in the screening-level financial comparison.

Category	Assumption	Description/Purpose
Electricity tariff	Phoenix: 0.10 $/kWh; Fairbanks: 0.08 $/kWh	Provides a flat energy-price comparison between the two climates.
Project life	20 years	Provides a common analysis period for all configurations.
Discount rate	5% real	Discounts future annual savings to present value.
Electricity-price escalation	2% real per year	Represents gradual growth in energy-cost savings over the project life.
Demand charges	Excluded	Avoids utility-specific billing structures in the base case.
Chiller CapEx	Estimated from rated cooling capacity and unit-cost assumptions	Provides a consistent capacity-based capital-cost comparison.
ATES CapEx	Includes simplified wellfield, pump, and heat-exchanger cost terms	Represents feasibility-level ATES cost screening, not site-specific design.
O&M cost	Estimated using simplified annual component-level O&M assumptions	Includes operating-cost differences without detailed maintenance contracts.
Economic metrics	Simple payback and discounted value of savings relative to the centrifugal baseline	Reports discounted savings and payback relative to the centrifugal baseline.

The annual cost of energy is calculated from the following:

$$C_{energy} = c_e E_{annual} \tag{22}$$

where c_e is the electricity tariff. The annual cost for operating the system is equal to the following:

$$C_{op} = C_{energy} + C_{O\&M} \tag{23}$$

The capital cost is calculated from assumptions at the component level, specifically for the chillers, piping, and ATES wells, pumps and heat exchangers. The incremental premium capital cost relative to the centrifugal baseline is as follows:

$$\Delta CapEx = CapEx_{alt} - CapEx_{base} \tag{24}$$

The first-year annual savings are calculated relative to the centrifugal baseline. For the MBC-only case, the implemented savings term includes energy-cost savings:

$$S_{1,MBC} = (E_{base} - E_{MBC})c_e \tag{25}$$

For the MBC+ATES case, the implemented savings term includes both energy-cost savings and the modeled O&M difference:

$$S_{1,ATES} = (E_{base} - E_{ATES})c_e + (C_{O\&M,base} - C_{O\&M,ATES}) \tag{26}$$

The present value of annual savings is calculated as follows:

$$PV_{sav} = \sum_{t=1}^{N} \frac{S_1(1+g)^{t-1}}{(1+r)^t} \tag{27}$$

where S_1 is the annual savings in the first year of operation considering the evaluated alternative, g is the real escalation rate, r is the real discount rate, and N is the lifespan of operating the system. The quantity PV_{sav} represents the discounted value of annual savings before subtracting the incremental capital cost.

The internal rate of return is calculated from the incremental premium and annual savings data:

$$\Delta CapEx = \sum_{t=1}^{N} \frac{S_1(1+g)^{t-1}}{(1+IRR)^t} \tag{28}$$

The simple payback period is equal to the following:

$$T_{pb} = \frac{\Delta CapEx}{S_1} \tag{29}$$

when $S_1 > 0$; otherwise, payback is undefined.

2.8. Model Verification and Quality Assurance

Model verification and quality-assurance checks were performed on the input data, hourly simulation outputs, dispatch logic, and financial calculations. These checks are intended to confirm that the model is internally consistent and that each cooling configuration is evaluated under comparable boundary conditions. They should not be interpreted as full empirical validation against measured data from an operating data center. These checks are summarized in Table 4. External reasonableness is instead assessed through the benchmarking discussion in Section 4.1.

Table 4. Model verification and quality-assurance checks.

Check Category	Verification Performed	Purpose
Time-series completeness	Each city uses 8760 hourly records for weather and load inputs.	Confirms complete annual simulations.
IT-load consistency	The same transformed server-load profile is used for Phoenix and Fairbanks.	Isolates climate and cooling-system effects.
Weather preprocessing	Hourly dry-bulb temperature and relative humidity are used to estimate wet-bulb conditions. Missing humidity values are filled by linear interpolation.	Avoids using dry-bulb temperature as a proxy for wet-bulb temperature.
Capacity matching	The centrifugal and magnetic bearing chiller cases use the same aggregate installed chiller capacity.	Prevents equipment sizing from biasing the comparison.
Physical bounds	Cooling loads, electrical power, flow fractions, ATES discharge, and ATES state of charge are constrained to non-negative values.	Prevents nonphysical hourly results.
ATES storage bounds	ATES state of charge is constrained between zero and the prescribed maximum storage capacity.	Ensures energy conservation within the simplified storage model.
Dispatch sequence	The hourly dispatch follows WSE, then ATES where applicable, then mechanical chiller operation.	Confirms that lower-energy cooling modes are used before compressor-based cooling.
Financial calculations	Escalation and discounting are applied once in the financial layer. All alternatives are compared relative to the centrifugal baseline.	Maintains a consistent economic comparison.

3. Results

The three cooling configurations were evaluated for Phoenix and Fairbanks using identical hourly IT load profiles and consistent operating assumptions. Results are presented for operating-mode duration, annual cooling electricity use, cooling-only PUE′, and economic performance relative to the centrifugal baseline. Although both cities use the same IT load profile, annual cooling electricity differs substantially because cooling-system operation is climate dependent. In Phoenix, the centrifugal baseline operates in Mode 3 for 6808 h. In Fairbanks, it operates in Mode 3 for 2113 h and in Mode 1 for 5350 h. Therefore, Fairbanks relies more heavily on WSE operation and less on compressor-based cooling. As a result, the centrifugal baseline requires 1169.4 MWh of annual cooling electricity in Phoenix and 361.6 MWh in Fairbanks.

The reported peak cooling-system electrical demand reductions are technical performance results. They are not monetized in the base-case financial analysis because demand charges, time-of-use tariffs, and grid-interconnection costs are outside the scope of the flat-tariff economic model.

Table 5 summarizes the main annual energy, cooling-only PUE′, and economic results for all configurations. The economic values for the MBC and MBC+ATES cases are reported relative to the centrifugal baseline.

Table 5. Summary comparison of cooling configurations in Phoenix and Fairbanks.

City	Configuration	Annual Cooling Electricity (MWh/yr)	Reduction vs. Baseline (%)	Average PUE′	Premium CapEx (USD)	Discounted Value of Savings (M USD)	Simple Payback (yr)
Phoenix	Centrifugal baseline	1169.4	–	1.095	–	–	–
	MBC	957.4	18.1	1.078	123,527	0.31	5.8
	MBC+ATES	961.6	17.8	1.078	534,940	0.99	7.9
Fairbanks	Centrifugal baseline	361.6	–	1.029	–	–	–
	MBC	319.4	11.7	1.026	123,527	0.05	36.6
	MBC+ATES	334.5	7.5	1.027	534,940	0.72	10.9

Note: PUE′ is the cooling-only power usage effectiveness metric defined in the Methods section. Premium CapEx, discounted value of savings, and simple payback are calculated relative to the centrifugal baseline.

3.1. Energy Performance

3.1.1. Operating Modes

Figure 2 shows the monthly distribution of operating modes for Phoenix. Mode 1 represents free cooling without chiller operation and occurs mainly during winter, accounting for 204 h annually. Mode 2 represents partial free cooling with supplemental mechanical cooling and lasts for 1748 h. Mode 3 represents mechanical cooling without WSE contribution and occurs for 6808 h. Under the modeled Phoenix weather conditions, mechanical cooling is required for most of the year.

Figure 3 shows the corresponding operating-mode distribution for Fairbanks. Mode 1 is the dominant operating condition and occurs for 5350 h annually. The system operates in Mode 2 for 1297 h and in Mode 3 for 2113 h. Compared with Phoenix, Fairbanks has substantially more hours of free cooling without chiller operation. Therefore, supplemental mechanical cooling is required for fewer hours.

In Figure 4, a comparison of the annual hours of operation in each mode is shown for both cities. The x-axis shows the study locations, and the stacked bars show annual operating hours by cooling mode. Phoenix has 6808 h in Mode 3, compared with 2113 h in Fairbanks. Conversely, Fairbanks has 5350 h in Mode 1, compared with 204 h in Phoenix. This difference in operating mode distribution provides the basis for the different energy and economic outcomes observed between the two climates.

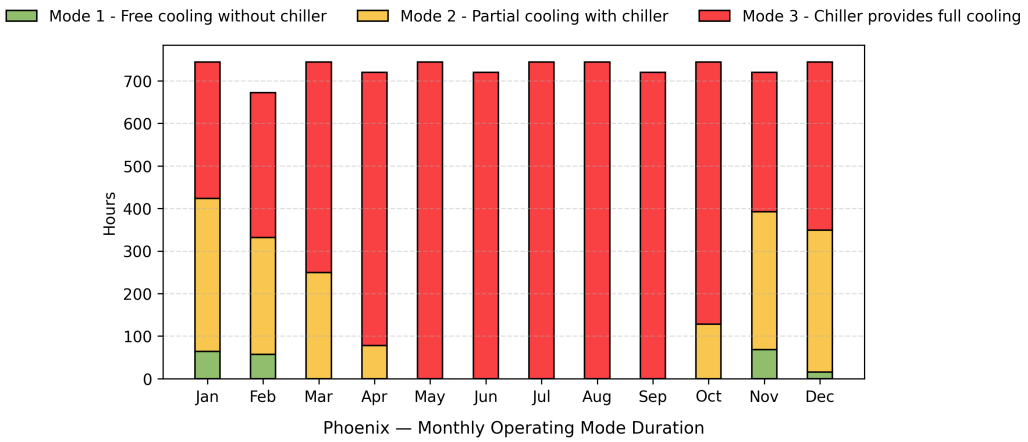


Figure 2. Monthly operating cooling mode duration for Phoenix, Arizona.

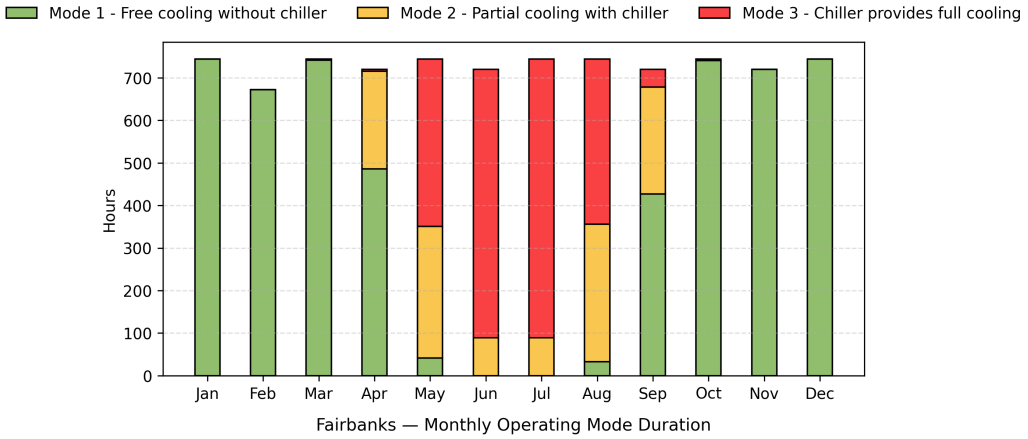


Figure 3. Monthly operating cooling mode duration for Fairbanks, Alaska.

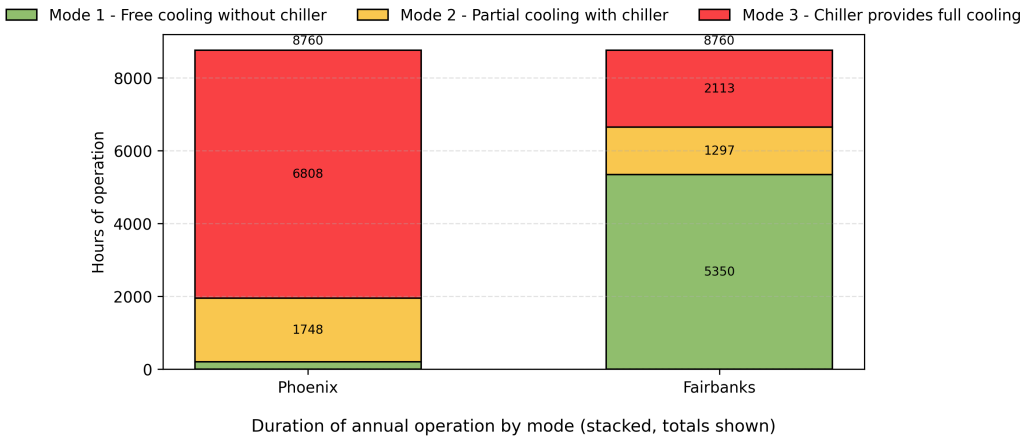


Figure 4. Comparison of annual cooling mode duration between Phoenix and Fairbanks.

3.1.2. Energy Consumption and PUE′

Figure 5 shows annual cooling electricity consumption and average cooling-only PUE′ for Phoenix. The centrifugal baseline consumes 1169.4 MWh of electricity annually. The MBC configuration reduces annual cooling electricity use to 957.4 MWh, corresponding to an 18.1% reduction relative to the baseline. The MBC+ATES configuration requires 961.6 MWh, corresponding to a 17.8% reduction. Average cooling-only PUE′ decreases from 1.095 for the centrifugal baseline to approximately 1.078 for both MBC-based configurations.

Figure 6 shows the same comparison for Fairbanks. The centrifugal baseline consumes 361.6 MWh of electricity annually. The MBC configuration reduces annual cooling electricity use to 319.4 MWh, corresponding to an 11.7% reduction. The MBC+ATES configuration consumes 334.5 MWh, corresponding to a 7.5% reduction relative to the baseline. Average cooling-only PUE′ is similar across the three configurations. It decreases from 1.029 for the centrifugal baseline to 1.026 for MBC and 1.027 for MBC+ATES.

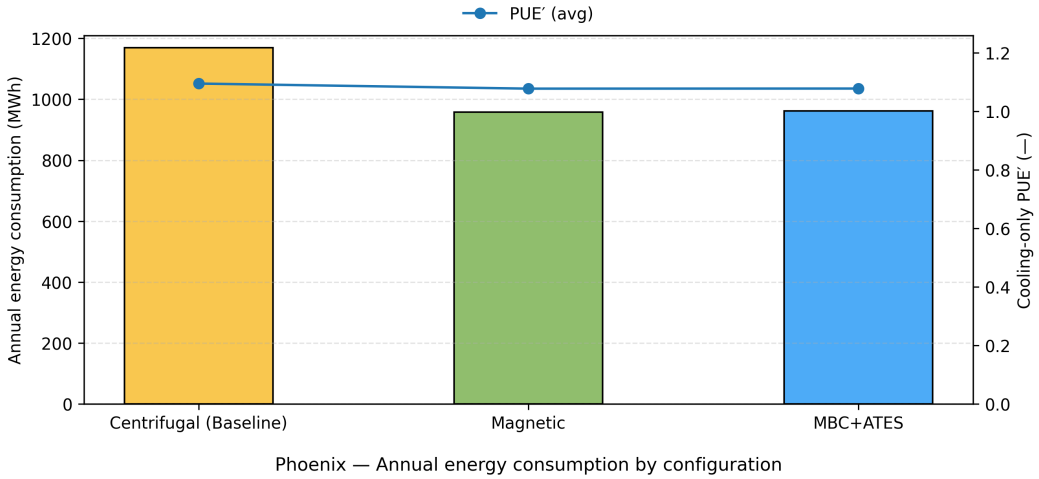


Figure 5. Annual cooling electricity consumption and corresponding average cooling-only PUE′ in Phoenix for each operating configuration.

Peak cooling-system electrical demand decreases by 119.4 kW in Phoenix and 71.6 kW in Fairbanks. These peak-demand reductions indicate a potential grid-capacity benefit. However, the base financial model does not assign monetary value to peak-demand reduction because demand charges and time-of-use pricing are not included in the flat-tariff assumptions.

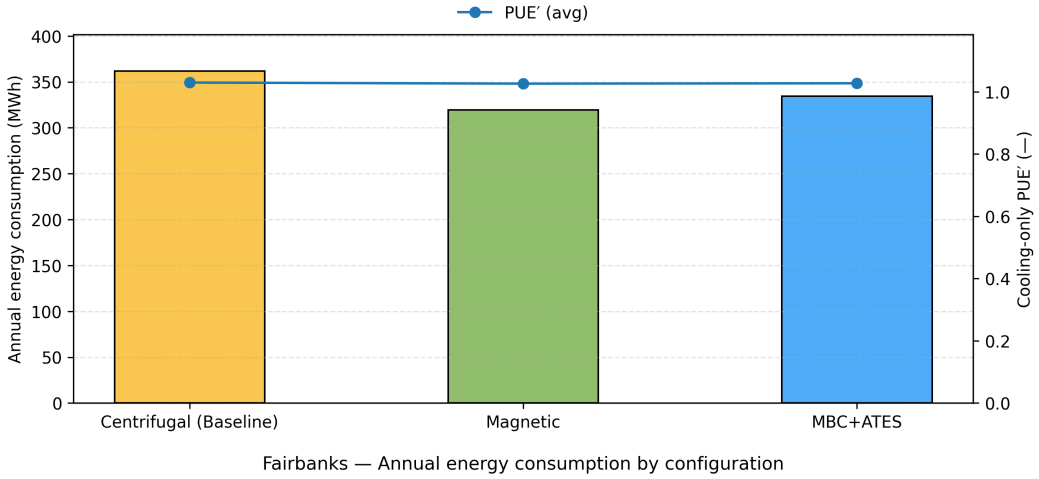


Figure 6. Annual cooling electricity consumption and corresponding average cooling-only PUE′ in Fairbanks for each operating configuration.

3.2. Economic Performance

Capital Cost, Operating Cost, and Payback

Figure 7 shows the economic metrics for Phoenix relative to the centrifugal baseline. The MBC case has an incremental capital cost of $123,527 and a simple payback period of 5.8 years. Its present value of savings, PV_{sav}, is $0.31 M. The MBC+ATES case has a

larger incremental capital cost of $534,940 and a longer simple payback period of 7.9 years. However, it has a higher PV_{sav} of $0.99 M under the modeled assumptions.

Figure 8 shows the corresponding economic metrics for Fairbanks. The MBC case has the same incremental capital cost of $123,527, but its simple payback period is longer at 36.6 years. Its present value of savings, PV_{sav}, is $0.05 M. The MBC+ATES case has an incremental capital cost of $534,940 and a simple payback period of 10.9 years. Its PV_{sav} is $0.72 M. Under the modeled tariff and operating assumptions, Fairbanks provides lower energy-cost savings from chiller replacement because it requires fewer annual mechanical-cooling hours.

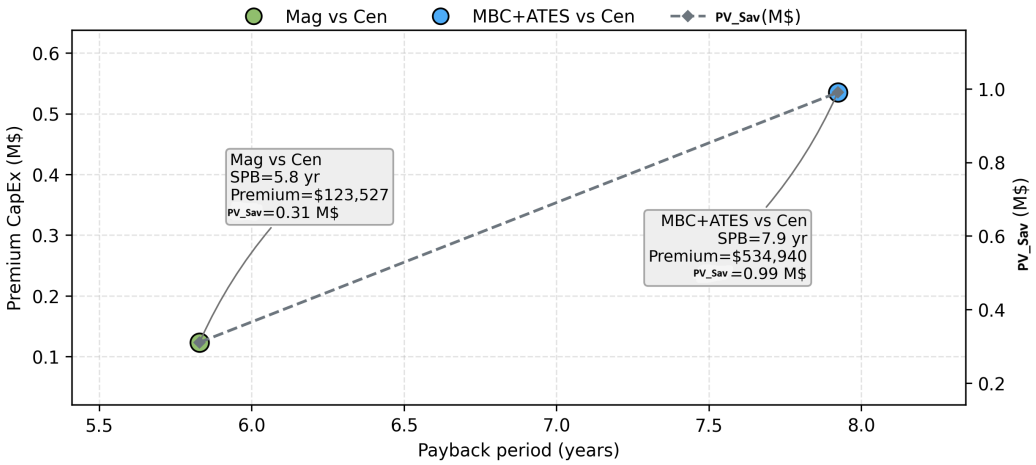


Figure 7. Simple payback period and premium CapEx with discounted savings for cooling for the City of Phoenix calculated relative to the centrifugal baseline.

The MBC+ATES case has slightly higher annual cooling electricity use than the MBC-only case in both cities. However, the economic comparison includes both electricity-cost savings and modeled O&M cost differences. This distinction is important because the additional electricity cost of MBC+ATES relative to MBC-only is small compared with the modeled O&M savings. In Phoenix, MBC+ATES uses 4.2 MWh/yr more than MBC-only, equal to approximately $420/yr at 0.10 $/kWh. In Fairbanks, MBC+ATES uses 15.1 MWh/yr more than MBC-only, equal to approximately $1,208/yr at 0.08 $/kWh. Therefore, the higher discounted value of savings for MBC+ATES is driven by the financial assumptions, especially the modeled O&M term, rather than by lower electricity consumption compared with MBC-only.

Because component-level maintenance contracts and vendor-specific O&M data were not available, the O&M costs used in this study should be interpreted as screening-level assumptions rather than itemized maintenance estimates. To show how strongly the MBC+ATES economic result depends on this assumption, Table 6 reports an illustrative O&M scenario check. The calculation uses the same energy costs, incremental CapEx, 20-year project life, 5% real discount rate, and 2% real escalation rate used in the base financial analysis. When the MBC+ATES O&M cost is set equal to the MBC-only O&M cost, the net present value becomes negative in both climates. This confirms that the economic advantage of MBC+ATES in the base case is conditional on the assumed O&M structure.

The MBC-only O&M cost used for the comparison is 102,360 USD/yr. For cases where the calculated simple payback exceeds the 20-year project life, the payback is reported as greater than 20 years. Cases with negative first-year savings do not have a meaningful simple payback period or positive IRR.

The energy results are held constant in this scenario check. Therefore, the changes in Table 6 are caused only by the assumed MBC+ATES O&M cost. This is important because MBC+ATES uses slightly more annual cooling electricity than MBC-only in the base simulations. The additional electricity use is 4.2 MWh/yr in Phoenix and 15.1 MWh/yr in Fairbanks, corresponding to approximately 420 USD/yr and 1208 USD/yr, respectively. These values are small relative to the assumed O&M difference. Therefore, the financial advantage of MBC+ATES in the base case is driven mainly by the O&M assumption rather than by additional energy savings relative to MBC-only.

Table 6. Illustrative O&M scenario check for the MBC+ATES case relative to the centrifugal baseline.

Metric	Base O&M	Same as MBC	25% Lower	25% Higher
Phoenix				
MBC+ATES O&M (USD/yr)	55,427	102,360	76,770	127,950
First-year savings (USD/yr)	67,713	20,780	46,370	−4,810
NPV (MUSD)	0.458	−0.230	0.145	−0.605
IRR (%)	13.0	−0.5	7.8	–
Payback (yr)	7.9	>20	11.5	–
Fairbanks				
MBC+ATES O&M (USD/yr)	55,451	102,360	76,770	127,950
First-year savings (USD/yr)	49,077	2,168	27,758	−23,422
NPV (MUSD)	0.185	−0.503	−0.128	−0.878
IRR (%)	8.5	−15.6	2.2	–
Payback (yr)	10.9	>20	19.3	–

Table 7 summarizes the expected direction of sensitivity for selected economic and operating assumptions. The final column provides a qualitative interpretation of likely effects on the economic ranking under otherwise unchanged base-case conditions. It should not be interpreted as a quantitative tornado analysis because it does not specify parameter ranges, interaction effects, climate-dependent responses, or re-optimized dispatch. Therefore, the reported economic ranking should be interpreted as conditional on the selected base-case assumptions rather than as a general ordering of MBC-only and MBC+ATES performance.

Table 7. Qualitative sensitivity of the economic ranking to selected base-case assumptions.

Parameter	Expected Effect on Results	Implication for Economic Ranking
Electricity tariff	Higher electricity prices change the value of annual energy savings.	Strengthens configurations with lower annual electricity use; may favor MBC-only when MBC+ATES has slightly higher electricity consumption.
Demand charges	Higher demand charges increase the value of reducing peak electrical demand.	May improve the relative economics of MBC+ATES if storage discharge reduces coincident peak chiller demand.
ATES capital cost	Higher ATES capital cost increases initial investment and reduces net present value.	Weakens MBC+ATES relative to MBC-only and lengthens simple payback.
O&M cost assumption	Higher annual O&M cost reduces annual net savings.	Strong driver of the ranking; when MBC+ATES O&M is set equal to MBC-only O&M, NPV becomes negative in both climates.
Well or storage discharge temperature	Lower discharge temperature improves cooling assistance, while higher temperature reduces useful cooling contribution.	Cooler storage discharge improves MBC+ATES performance; warmer discharge weakens it.
Usable storage capacity	Greater usable storage can increase discharge assistance but may also require higher capital cost.	Economic benefit depends on the balance between avoided chiller operation, peak-demand reduction, and added ATES cost.

The economic ranking is, therefore, conditional on the selected base-case technical and financial assumptions, as summarized qualitatively in Table 7.

Energy costs are calculated using flat electricity tariffs of 0.10 $/kWh for Phoenix and 0.08 $/kWh for Fairbanks. Incremental CapEx, first-year savings, discounted savings, net present value, IRR, and simple payback are reported relative to the centrifugal baseline. The discounted savings column corresponds to the present value of savings before subtracting incremental CapEx. Net present value is calculated as discounted savings minus incremental CapEx.

A detailed breakdown of the capital cost, annual operating cost, annual savings, discounted savings, net present value, internal rate of return, and simple payback period for all configurations is provided in Table 8.

Table 8. Detailed economic breakdown for the cooling configurations in Phoenix and Fairbanks.

Metric	Phoenix Centrifugal Baseline	Phoenix MBC	Phoenix MBC+ATES	Fairbanks Centrifugal Baseline	Fairbanks MBC	Fairbanks MBC+ATES
Total CapEx (USD)	2,047,193	2,170,720	2,582,133	2,047,193	2,170,720	2,582,133
Incremental CapEx (USD)	–	123,527	534,940	–	123,527	534,940
Annual energy cost (USD/yr)	116,940	95,740	96,160	28,928	25,552	26,760
Annual O&M cost (USD/yr)	102,360	102,360	55,427	102,360	102,360	55,451
Total annual operating cost (USD/yr)	219,300	198,100	151,587	131,288	127,912	82,211
First-year savings (USD/yr)	–	21,200	67,713	–	3,376	49,077
Discounted savings (M USD)	–	0.31	0.99	–	0.05	0.72
Net present value (M USD)	–	0.19	0.46	–	-0.07	0.18
IRR (%)	–	18.0	13	–	-3.0	8.5
Simple payback (yr)	–	5.8	7.9	–	36.6	10.9

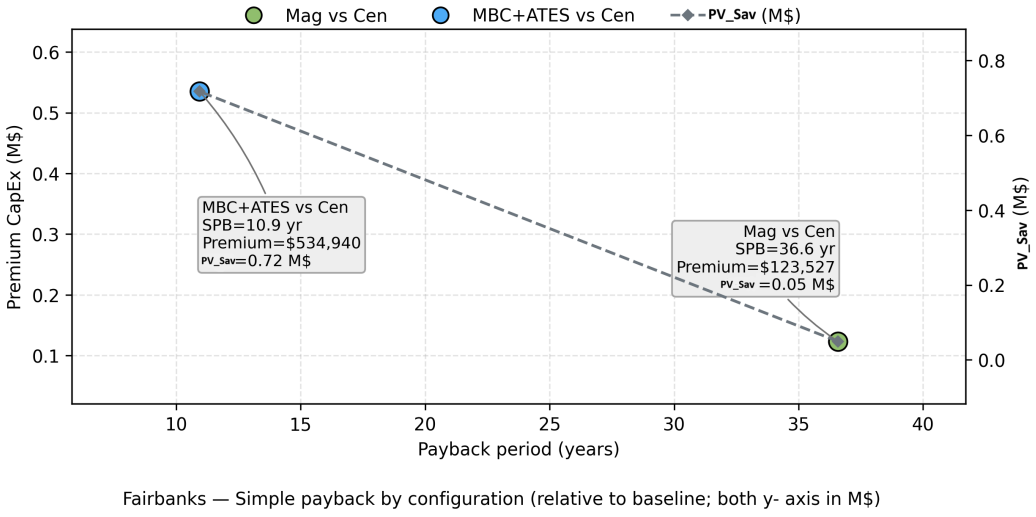


Figure 8. Simple payback period and premium CapEx with discounted savings for cooling configurations in Fairbanks relative to the centrifugal baseline.

4. Discussion

The economic results should be interpreted separately from the electricity-consumption results. The MBC-only case has the lowest annual cooling electricity use in both climates, while the MBC+ATES case has slightly higher electricity use because the modeled ATES operation adds pumping energy and is limited by the prescribed storage assumptions. The higher discounted value of savings for MBC+ATES is, therefore, driven by the modeled O&M cost difference rather than by additional electricity savings relative to MBC-only. Accordingly, MBC+ATES should not be described as generally more economically attrac-

tive than MBC-only; its apparent economic advantage in this study is conditional on the selected screening-level assumptions.

The economic ranking is, therefore, conditional on the assumed tariff, capital cost, O&M cost, project life, and simplified ATES representation. The result should not be interpreted as evidence that MBC+ATES is more energy efficient than MBC-only. Rather, it shows that the financial outcome can differ from the energy outcome when non-energy cost terms are included. Accordingly, MBC+ATES should not be described as generally more economically attractive than MBC-only; its apparent economic advantage in this study is a conditional result of the selected screening-level O&M assumptions.

Using hourly relative humidity data improved the representation of cooling-tower and WSE operation. In Phoenix, lower relative humidity increases the potential for evaporative cooling during some hours. However, high outdoor temperatures still limit the availability of full free cooling. In Fairbanks, lower outdoor temperatures provide more free-cooling hours despite higher relative humidity. These results show why cooling technologies should be evaluated using wet-bulb conditions rather than dry-bulb temperature alone.

Annual cooling electricity use is lower for the MBC case in both climates. However, the relative benefit is larger when compressor operation is more frequent. This is expected because MBC energy savings occur only during hours when the mechanical chiller operates. When a larger share of the annual cooling load is met by the WSE, the chiller operates less often. As a result, improved chiller efficiency has a smaller effect on total annual cooling electricity use. Similar climate dependence has been reported for free-cooling and ATES-supported cooling systems, where annual performance depends strongly on ambient conditions and seasonal operating patterns [10,13].

In the base-case simulations, the MBC+ATES configuration has similar but slightly higher annual cooling electricity use than the MBC-only case. This result reflects the screening-level ATES representation used in this study. The model includes finite initial storage, discharge-assisted operation, hydraulic pumping power, and prescribed storage parameters. It does not include optimized seasonal charging. Under these assumptions, ATES can offset part of the chiller load during selected hours, but pumping energy and storage constraints reduce the net electricity benefit. Therefore, the MBC+ATES results should be interpreted as a screening-level storage-assisted cooling case and not as a full techno-economic assessment of seasonal ATES deployment.

The monthly operating-mode figures provide the temporal comparison of WSE and chiller operation, while the annual energy and economic tables summarize the resulting performance metrics. A more detailed hourly ATES dispatch plot was not added because the ATES case is represented as a screening-level storage-assisted configuration rather than an optimized seasonal storage system. Within this simplified representation, ATES discharge can reduce chiller load during selected hours, but the added pumping power and finite storage constraints offset part of this benefit. This explains why MBC+ATES has slightly higher annual cooling electricity use than MBC-only, while the economic indicators remain more favorable under the modeled O&M assumptions.

The economic results are also sensitive to cooling-system operating hours and financial assumptions. In Phoenix, the greater use of mechanical cooling creates larger energy-cost savings from chiller replacement. This leads to shorter payback periods than in Fairbanks for the MBC-only case. In Fairbanks, the smaller energy-saving opportunity lengthens the MBC-only payback. The MBC+ATES result is influenced by both energy savings and modeled O&M assumptions. Therefore, the economic ranking should be interpreted within the assumed tariff, capital cost, O&M cost, and project life. Additional indirect economic benefits, such as reduced indirect water use from electricity generation, are outside the scope of this work.

4.1. Benchmarking Against Previous Studies

The modeled trends are consistent with previous studies, but they should be interpreted as a reasonableness check rather than direct validation. The model predicts larger MBC benefits in Phoenix than in Fairbanks because Phoenix has more hours requiring mechanical cooling. This trend is consistent with prior work showing that magnetic bearing chiller savings depend on climate, condenser-water conditions, and the number of hours requiring compressor operation [9]. The reduced value of chiller replacement in Fairbanks is also consistent with the broader finding that free-cooling availability strongly affects annual data-center cooling energy use.

For the ATES case, the model shows that storage performance depends on storage size, pumping power, and operating assumptions. This is consistent with ATES techno-economic studies that identify storage design, hydrogeology, pumping energy, capital cost, and operating strategy as major drivers of performance and cost [11–13,15].

4.2. Limitations and Future Work

Several limitations should be considered when interpreting these results. First, the economic analysis uses flat electricity tariffs for Phoenix and Fairbanks. Demand charges, time-of-use rates, utility incentives, tax effects, financing structure, and grid-interactive operation are not included. These factors could affect the economic ranking of the cooling configurations, especially for systems that reduce or shift peak electrical demand. The study does not quantify direct cooling-water consumption, cooling-tower makeup water, evaporative losses, blowdown, or indirect water use associated with electricity generation. These water-related effects should be evaluated in future work using site-specific water-source, cooling-system, and grid-water-intensity data.

Second, the ATES case is represented as a screening-level storage-assisted cooling configuration. The model uses prescribed values for storage capacity, well temperatures, well depth, flow rate, and standing loss. It does not include a site-specific groundwater-flow or heat-transport model. It also does not represent ATES charging, cyclic seasonal operation, or optimized charge/discharge control. These simplifications are important because ATES performance depends on hydrogeological conditions, pumping energy, storage design, and operating strategy [1,11,13,15]. Therefore, the MBC+ATES results should be interpreted as hypothetical screening results rather than evidence of actual deployability in Phoenix or Fairbanks. A site-feasibility study would require local aquifer properties, groundwater-flow conditions, allowable extraction and injection rates, water chemistry, thermal recovery efficiency, and regulatory constraints.

Third, the IT load profile is a transformed representative server-load profile rather than a measured load trace from a specific data center. The source profile is used only to provide normalized hourly variation, and it is rescaled with an 80% minimum load to represent high-load-factor data-center operation. The same profile is used for both cities to isolate climate and cooling-system effects. This assumption supports a controlled comparison, but it does not capture the full range of possible data-center operating patterns.

Fourth, the model was verified through internal quality-assurance checks and benchmarked against trends reported in the literature. However, measured operating data for the exact cooling configurations were not available. Therefore, the results should be interpreted as verified screening-level simulations rather than as a calibrated facility model.

Future work should extend the analysis in several directions. A full seasonal ATES model should include charging, discharging, cyclic storage balance, and optimized control. Site-specific hydrogeological modeling should evaluate aquifer feasibility, well spacing, thermal recovery, and groundwater constraints. Sensitivity analysis should also be performed for key technical and economic parameters. These parameters include electricity

tariff, demand charges, ATES storage capacity, pumping head, well temperature, chiller cost, O&M cost, time-of-use rates, negotiated tariffs, power purchase agreements, capacity-related costs, discount rate, and IT-load profile.

The O&M scenario check included in the present revision addresses the dominant economic driver identified in this study; however, a broader multi-parameter sensitivity analysis remains necessary to evaluate the combined effects of electricity tariff, demand charges, ATES capital cost, pumping head, storage capacity, well temperature, discount rate, and IT-load profile. Future studies should also compare the model against measured data from operating data centers or detailed calibrated building-energy simulations. Future work should evaluate alternative IT-load profiles, including flatter hyperscale operation, AI-training-dominated operation, and more variable enterprise data-center operation, to quantify how load-shape assumptions affect cooling energy and economic results.

5. Conclusions

This study developed a comparative techno-economic framework for three data-center cooling configurations. The configurations were a centrifugal chiller baseline, a magnetic bearing chiller (MBC) system, and an MBC system integrated with aquifer thermal energy storage (ATES). The analysis used hourly simulations for Phoenix and Fairbanks. Both cities were evaluated with identical IT load profiles, equal aggregate installed chiller capacity, humidity-based wet-bulb calculations, and consistent operating assumptions.

The key findings are summarized as follows:

- The MBC configuration reduced annual cooling electricity consumption relative to the centrifugal baseline in both climates. It also improved the cooling-only power usage effectiveness, PUE′. The reduction was larger in Phoenix because the cooling system relied more heavily on mechanical cooling.
- The screening-level MBC+ATES configuration reduced annual cooling electricity use relative to the centrifugal baseline. However, it did not provide additional electricity savings relative to the MBC-only case in the base-case simulations. This case should be interpreted only as a simplified discharge-assisted cold-storage screening scenario, not as a complete seasonal ATES design or a full techno-economic assessment of seasonal ATES deployment. The model does not include seasonal charging, cyclic annual storage operation, thermal recovery, or site-specific aquifer heat-transport modeling. Under this limited representation and the assumed O&M cost structure, MBC+ATES produced a higher discounted value of savings than MBC-only. However, the O&M scenario check shows that when MBC+ATES O&M is set equal to MBC-only O&M, the NPV becomes negative in both climates, indicating that the apparent economic advantage of MBC+ATES is strongly conditional on the assumed O&M cost structure. This financial result should not be interpreted as a general conclusion that ATES improves data-center cooling economics in all locations or system designs.
- Economic performance was influenced by cooling energy savings, local electricity tariffs, capital cost, operation and maintenance (O&M) assumptions, and project life. Under the modeled assumptions, the MBC case had a shorter payback period in Phoenix than in Fairbanks. The MBC+ATES case produced a higher discounted value of savings than MBC-only in both cities, but required greater initial capital investment.

Overall, the results are specific to the modeling assumptions, input data, and system configurations used in this study. They should be interpreted as comparative outcomes within the defined modeling framework. They should not be treated as site-specific design recommendations without additional hydrogeological assessment, tariff analysis, and sensitivity testing.

Supplementary Materials: The following supporting information can be downloaded at: https://www.mdpi.com/article/10.3390/en19173947/s1, Workbook S1: PHOENIX_DataCenter_Profile.xlsx, processed hourly input profile for Phoenix including date/time, server load, indoor wet-bulb temperature, outdoor dry-bulb temperature, and relative humidity; Workbook S2: FAIRBANKS_DataCenter_Profile.xlsx, processed hourly input profile for Fairbanks including date/time, server load, indoor wet-bulb temperature, outdoor dry-bulb temperature, and relative humidity.

Author Contributions: Conceptualization, A.M., A.S. and U.P.; methodology, A.M.; software, A.M.; Validation (internal model checks), A.M., A.S., C.B. and U.P.; formal analysis, A.M.; investigation, A.M.; resources, A.M., A.S. and U.P.; data curation, A.M.; writing—original draft preparation, A.M.; writing—review and editing, A.M., Y.-F.L., A.S., C.B. and U.P.; visualization, A.M.; supervision, Y.-F.L., A.S., U.P. and C.B.; project administration, A.M., A.S., U.P., Y.-F.L. and C.B. All authors have read and agreed to the published version of the manuscript.

Funding: This research was funded under the provisions of section 104 of the Water Resources Research Act annual base grants (104b) program made possible and distributed through the Illinois Water Resources Center and the U.S. Geological Survey. The funding provided paid for the publication costs.

Data Availability Statement: The weather and reference-building datasets analyzed in this study are available from the publicly accessible sources cited in the manuscript. The original contributions presented in this study are included in the article and supplementary material. The processed data and simulation code generated during the study is part of an ongoing research workflow and can be made available from the corresponding author upon reasonable request.

Conflicts of Interest: The authors declare no conflicts of interest.

Abbreviations and Symbols

Abbreviations and symbols used in this study:

Term or Symbol	Definition
AI	Artificial intelligence
ASHRAE	American Society of Heating, Refrigerating and Air-Conditioning Engineers
ATES	Aquifer thermal energy storage
CapEx	Capital expenditure
COP	Coefficient of performance
CRAH	Computer room air handler
DOE	U.S. Department of Energy
HVAC	Heating, ventilation, and air conditioning
IRR	Internal rate of return
IT	Information technology
MBC	Magnetic bearing chiller
NPV	Net present value
O&M	Operation and maintenance
OpEx	Operating expenditure
PUE′	Cooling-only power usage effectiveness used in this study
RH	Relative humidity
SPB	Simple payback period
UTES	Underground thermal energy storage
WSE	Water-side economizer
C_{energy}	Annual electricity cost for cooling
$C_{O\&M}$	Annual operation and maintenance cost
C_{op}	Annual operating cost
c_e	Electricity tariff

$C_{\min,h}$	Smaller heat-capacity rate of the chilled-water and condenser-water streams at hour h
E_{annual}	Annual cooling electricity consumption
E_h	Stored thermal energy at hour h
$E_{\max}$	Maximum storage energy capacity
g	Annual electricity-price escalation rate
N	Project life
$P_{IT,h}$	IT electrical load at hour h
P_{min}	Minimum modeled IT load
P_{peak}	Peak modeled IT load
$P_{raw,h}$	Original hourly reference-building load
PV_{sav}	Present value of annual savings
$Q_{IT,h}$	IT heat load at hour h
$Q_{sum,h}$	Total hourly cooling load
$Q_{wse,h}$	Cooling rate provided by the water-side economizer at hour h
r	Real discount rate
S_1	First-year annual savings
$T_{ctw,h}$	Condenser/tower-water temperature at hour h
$T_{ctw,min}$	Minimum allowed condenser/tower-water temperature
$T_{cw,r,h}$	Return chilled-water temperature at hour h
T_{db}	Dry-bulb temperature
T_{pb}	Simple payback period
T_{wb}	Wet-bulb temperature
$T_{wb,out,h}$	Outdoor wet-bulb temperature at hour h
$\Delta CapEx$	Incremental premium capital cost relative to the baseline
ΔT_{app}	Cooling-tower approach temperature
ε_h	Heat-exchanger effectiveness at hour h

References

1. Oh, H.; Jin, W.; Peng, P.; Winick, J.; Sickinger, D.; Sartor, D.; Zhang, Y.; Beckers, K.; Kitz, K.; Acero-Allard, D.; Atkinson, T. Techno-Economic Performance of Reservoir Thermal Energy Storage for Data Center Cooling Systems. *Appl. Energy* **2025**, *391*, 125858. [CrossRef]
2. McKinsey & Company. Global Energy Perspective 2024; 2024. Available online: https://www.mckinsey.com/industries/energy-and-materials/our-insights/global-energy-perspective (accessed on 3 March 2026).
3. Lee, V.; Seshadri, P.; O'Niell, C.; Choudhary, A.; Holstege, B.; Deutscher, S.A. Breaking Barriers to Data Center Growth; Boston Consulting Group, 2025. Available online: https://www.bcg.com/publications/2025/breaking-barriers-data-center-growth (accessed on 21 February 2026).
4. Newmark Research. 2025 United States Data Center Market Outlook; Technical Report, 2025. Available online: https://www.nmrk.com/insights/market-report/2025-us-data-center-market-outlook (accessed on 5 January 2026).
5. Siddik, M.A.B.; Shehabi, A.; Marston, L. The Environmental Footprint of Data Centers in the United States. *Environ. Res. Lett.* **2021**, *16*, 064017. [CrossRef]
6. Mytton, D. Data Centre Water Consumption. *npj Clean Water* **2021**, *4*, 11. [CrossRef]
7. Lei, N.; Lu, J.; Shehabi, A.; Masanet, E. The Water Use of Data Center Workloads: A Review and Assessment of Key Determinants. *Res. Conserv. Recyc.* **2025**, *219*, 108310. [CrossRef]
8. The Green Grid. Water Usage Effectiveness (WUE): A Green Grid Data Center Sustainability Metric; White Paper 35, 2011. Available online: https://archive.thegreengrid.org/en/resources/library-and-tools/238-WP (accessed on 14 December 2025).
9. Dai, Y.; Chen, X.; Zhang, L. Energy-Saving and Economic Analysis of the Data Center Cooling System Using Magnetic Bearing Chillers under Different Climate Conditions. *Case Stud. Thermal Eng.* **2024**, *61*, 104915. [CrossRef]
10. Fleuchaus, P.; Godschalk, B.; Stober, I.; Blum, P. Worldwide Application of Aquifer Thermal Energy Storage—A Review. *Renew. Sustain. Energy Rev.* **2018**, *94*, 861–876. [CrossRef]
11. Schüppler, S.; Fleuchaus, P.; Blum, P. Techno-Economic and Environmental Analysis of an Aquifer Thermal Energy Storage (ATES) in Germany. *Geotherm. Energy* **2019**, *7*, 11. [CrossRef]

12. Herrmann, M.; Fleuchaus, P.; Godschalk, B.; Verbiest, M.; Sørensen, S.N.; Blum, P. Capital Costs of Aquifer Thermal Energy Storage (ATES): A Review. *Renew. Sustain. Energy Rev.* **2026**, *226*, 116202. [CrossRef]
13. Dvorak, V.; Zavrel, V.; Torrens Galdiz, J.I.; Hensen, J.L. Simulation-Based Assessment of Data Center Waste Heat Utilization Using Aquifer Thermal Energy Storage. *Build. Simul.* **2020**.. [CrossRef]
14. Zhang, Y.; Acero-Allard, D.; Atkinson, T.; Beckers, K.; Dobson, P.; Jin, W.; Lei, N.; Oh, H.; Peng, P.; Sartor, D.; Sickinger, D. Addressing Data Center Cooling Needs through the Use of Subsurface Thermal Energy Storage Systems. In Proceedings of the SPE Energy Transition Symposium, Houston, Texas, USA, 22–23 August 2023. [CrossRef]
15. Winick, J.A.; Zhu, G.; Kitz, K.; Adams, A. Reducing Data Center Peak Cooling Demand and Energy Costs with Underground Thermal Energy Storage (UTES). In Proceedings of the 50th Workshop on Geothermal Reservoir Engineering, Stanford University, Stanford, CA, USA, 10–12 February 2025.
16. Pandey, U.; Stumpf, A.J.; Lin, Y.-F.F. Aquifer Thermal Energy Storage: Groundwater for Efficient Data Center Cooling in the United States. *Groundwater*, **2026**, *64*, 394–404. [CrossRef] [PubMed]
17. Jackson, M.D.; Regnier, G.; Staffell, I. Aquifer Thermal Energy Storage for Low Carbon Heating and Cooling in the United Kingdom: Current Status and Future Prospects. *Appl. Energy* **2024**, *376*, 124096. [CrossRef]
18. Kleyböcker, A.; Bloemendal, M. ATES Factsheet; Water Europe, 2020. Available online: https://mp.watereurope.eu/media/factsheets/$Factsheet_ATES_V5_ypLKKy4.pdf$ (accessed on 26 April 2026).
19. Ever-Green Energy. *ATES Feasibility Study—St. Paul Ford Site*; Technical Report, 2016. Available online: https://www.stpaul.gov/departments/planning-and-economic-development/planning/highland-bridge/ford-site-zoning-and-2 (accessed on 21 August 2026).
20. WeatherSpark. Historical Weather during 2022—Phoenix, Arizona, USA. Available online: https://weatherspark.com/h/y/2460/2022/Historical-Weather-during-2022-in-Phoenix-Arizona-United-States (accessed on 20 August 2026).
21. WeatherSpark. Historical Weather during 2022–Fairbanks, Alaska, USA. Available online: https://weatherspark.com/h/y/273/2022/Historical-Weather-during-2022-in-Fairbanks-Alaska-United-States (accessed on 20 August 2026).
22. Weather Underground. Phoenix, Arizona Weather History, Phoenix Sky Harbor International Airport (KPHX), 2022. Available online: https://www.wunderground.com/history/monthly/us/az/phoenix/KPHX/date/2022-1 (accessed on 11 May 2026).
23. Weather Underground. Fort Wainwright, Alaska Weather History, Ladd Army Airfield (PAFB), 2022. Available online: https://www.wunderground.com/history/monthly/us/ak/fort-wainwright/PAFB/date/2022-1 (accessed on 11 May 2026).
24. Stull, R. Wet-Bulb Temperature from Relative Humidity and Air Temperature. *J. Appl. Meteorol. Climatol.* **2011**, *50*, 2267–2269. [CrossRef]
25. Buck, A.L. New Equations for Computing Vapor Pressure and Enhancement Factor. *J. Appl. Meteorol.* **1981**, *20*, 1527–1532. [CrossRef]
26. ASHRAE. *ASHRAE Handbook—Fundamentals*; ASHRAE: Peachtree Corners, GA, USA, 2021.
27. U.S. Department of Energy, OpenEI. Hospital Building Electricity Load Profile Data (Commercial Reference Building Dataset). Available online: https://data.openei.org/submissions/153 (accessed on 20 July 2026).
28. ASHRAE. *ASHRAE Handbook—HVAC Systems and Equipment*; ASHRAE: Peachtree Corners, GA, USA, 2020.

Disclaimer/Publisher's Note: The statements, opinions and data contained in all publications are solely those of the individual author(s) and contributor(s) and not of MDPI and/or the editor(s). MDPI and/or the editor(s) disclaim responsibility for any injury to people or property resulting from any ideas, methods, instructions or products referred to in the content.